Pharm Res (2012) 29:1232–1241
DOI 10.1007/s11095-012-0675-y

RESEARCH PAPER

Formulation and *In Vitro* Characterization of Composite Biodegradable Magnetic Nanoparticles for Magnetically Guided Cell Delivery

Michael Chorny • Ivan S. Alferiev • Ilia Fishbein • Jillian E. Tengood • Zoë Folchman-Wagner • Scott P. Forbes • Robert J. Levy

Received: 3 August 2011 / Accepted: 4 January 2012 / Published online: 25 January 2012

ABSTRACT

Purpose Cells modified with magnetically responsive nanoparticles (MNP) can provide the basis for novel targeted therapeutic strategies. However, improvements are required in the MNP design and cell treatment protocols to provide adequate magnetic properties in balance with acceptable cell viability and function. This study focused on select variables controlling the uptake and cell compatibility of biodegradable polymer-based MNP in cultured endothelial cells.

Methods Fluorescent-labeled MNP were formed using magnetite and polylactide as structural components. Their magnetically driven sedimentation and uptake were studied fluorimetrically relative to cell viability in comparison to non-magnetic control conditions. The utility of surface-activated MNP forming affinity complexes with replication-deficient adenovirus (Ad) for transduction achieved concomitantly with magnetic cell loading was examined using the green fluorescent protein reporter.

Results A high-gradient magnetic field was essential for sedimentation and cell binding of albumin-stabilized MNP, the latter being rate-limiting in the MNP loading process. Cell loading up to 160 pg iron oxide per cell was achievable with cell viability >90%. Magnetically driven uptake of MNP-Ad complexes can provide high levels of transgene expression potentially useful for a combined cell/gene therapy.

Conclusions Magnetically responsive endothelial cells for targeted delivery applications can be obtained rapidly and efficiently using composite biodegradable MNP.

M. Chorny • I. S. Alferiev • I. Fishbein • J. E. Tengood • Z. Folchman-Wagner • S. P. Forbes • R. J. Levy
Division of Cardiology
The Children's Hospital of Philadelphia
Philadelphia, Pennsylvania 19104, USA

M. Chorny (✉)
The Children's Hospital of Philadelphia
Abramson Research Building
Suite 702 G, 3615 Civic Center Boulevard
Philadelphia, Pennsylvania 19104-4318, USA
e-mail: chorny@email.chop.edu

KEY WORDS biodegradable nanoparticle · cell therapy · magnetic targeting · restenosis · stent angioplasty · vascular disease

ABBREVIATIONS

Ad	adenovirus
BAEC	bovine aortic endothelial cells
BSA	bovine serum albumin
CAR	Coxsackie-adenovirus receptor
CMV	cytomegalovirus
DCC	1,3-dicyclohexylcarbodiimide
DMEM	Dulbecco's modification of Eagle's medium
EDC	1-ethyl-3-(3-dimethylaminopropyl)carbodiimide
FBS	fetal bovine serum
GFP	green fluorescent protein
MNP	magnetic nanoparticle
PBS	phosphate buffered saline
PLA	polylactide
SPDP	N-succinimidyl 3-(2-pyridyldithio)propionate

INTRODUCTION

Cells impregnated with magnetic nanoparticles (MNP) are being explored for a range of therapeutic and diagnostic applications, including magnetic resonance imaging (1,2), magnetically driven endothelialization of vascular grafts and injured blood vessels (3–7), vascular tissue engineering (8), and cancer treatment (9). Introduction and implementation of these strategies in clinical practice essentially depends on identification and optimization of MNP formulation characteristics and variables in the cell loading process affecting the magnetic properties, viability and functionality of the cells post modification, which in turn requires a better understanding of the physical and cellular mechanisms underlying the MNP-cell interactions.

The design of MNP suitable for preparing magnetically responsive cells for targeted delivery applications poses a number of challenges. In order to be effective, MNP-modified cells should have sufficient magnetic susceptibility for their guidance and concentration at a target site. At the same time, the amount of MNP providing adequate magnetic responsiveness should not adversely affect the cell viability and capacity for substrate attachment, which is essential for their homing and retention in the region of interest post delivery. The process of cell loading with MNP should be rapid and MNP dose-efficient. Some applications may require additional modifications of the MNP formulations and loading process to provide cells traceable and quantifiable by fluorescent imaging or expressing high levels of therapeutically relevant transgenes for combination (gene/cell delivery) strategies (10). The characteristics and design of a MNP formulation may also require optimization depending on specific cell type. Standard commercially available iron oxide formulations, while not being ideally suited for generating fully functional and strongly magnetically responsive cells, also show significant variability in a wide range of properties, including size, morphology and surface chemistry (11), and thus may not allow systematic investigation of specific formulation variables determining the efficiency of the cell loading process.

This study is concerned with the design and characterization of biodegradable MNP formulations suitable for preparing magnetically responsive cells for targeted vascular delivery. We previoulsy reported a composite, polylactide (PLA)-based MNP formulation enabling efficient loading of endothelial cells and applied for their magnetic targeting to injured blood vessels in the rat carotid stenting model (7). In the current study the formulation procedure was modified to provide two types of strongly magnetically responsive and fully biodegradable, fluorescent-labeled MNP with different average sizes and narrow size distributions. The kinetics of their cell uptake were investigated in comparison to the respective sedimentation rates in order to identify the rate-limiting component of the magnetic cell loading process. The viability and capacity for cell-substrate attachment were examined in MNP-loaded cells to determine the threshold of MNP internalization achievable with acceptable cell compatibility. Additionally, a novel PLA-based formulation enabling MNP loading accomplished simultaneously with magnetically enhanced adenoviral transduction was characterized in terms of its cell uptake and gene transfer efficiency.

MATERIALS AND METHODS

Materials

Poly(D,L-lactide) (Mw 75,000–120,000), ferric chloride hexahydrate, ferrous chloride tetrahydrate, sodium hydroxide, oleic acid, polyallylamine hydrochloride with an average number molecular weight of 8,500–11,000, and bovine serum albumin (BSA) were obtained from Sigma-Aldrich (MO, USA). A succinimidyl ester of BODIPY$_{564/570}$ was purchased from Invitrogen (CA, USA). N-succinimidyl 3-(2-pyridyldithio)propionate (SPDP) was purchased from Thermo Scientific Pierce Protein Research Products (IL, USA). Type 5 replication-deficient adenovirus (Ad) encoding green fluorescent protein (GFP) under the control of CMV promoter ($_{GFP}$Ad) was obtained from the Gene Vector Core Facility of the University of Pennsylvania. The human recombinant D1 domain of the Coxsackie-Ad receptor (CAR) was prepared as described elsewhere (12).

Polyallylamine-derived surface-active agent (PAA-Chol-PDT-SO_3^-) for surface functionalization of MNP used for magnetically driven transduction experiments (See below), was synthesized by acylation of polyallylamine base (degree of polymerization, n=100) at 0°C in a mixture of dichloromethane and 2-propanol (2:1 by volume) with N-succinimidyl esters of the corresponding acids to provide the polymer with pendant 3-(2-pyridyldithio)propionyl, β-cholesteryloxyacetyl and sulfoacetyl (as a tetraethylammonium salt) residues. The amounts of the esters were adjusted to provide the molar ratio of 4:1:3 between the respective functional groups. To prevent decomposition of the 2-pyridyldithio residues by uncapped amino groups of polyallylamine and assure their complete acylation, SPDP was added in excess toward the end of the reaction. The resulting polymer was precipitated by replacement of the solvents with ethyl acetate. The excess of SPDP and the non-polymeric byproducts (mostly N-hydroxysuccinimide) were removed by washing with ethyl acetate – *tert*-butanol (1:1) followed by ethyl acetate. ^{1}H NMR of the polymer (400 MHz, $CDCl_3$-CD_3OD, 2:1) confirmed the incorporation of all functional groups. The protons of 2-pyridyldithio group appear at δ 8.4, 7.8 and 7.1 ppm (1:2:1), β-cholesteryloxyacetyl residues display distinct signals at δ 5.3 ppm (OCH_2CO), 0.6 and 0.8 ppm (different CH_3). The incorporation of sulfoacetyl residues was confirmed based on the signals of their counter-cation protons at δ 1.3 ppm (CH_3) and 3.2 ppm (CH_2). Polyallylamine base was prepared from polyallylamine hydrochloride by treating it in aqueous solution with the strongly basic anionite Dowex G-55 (OH-form), followed by water replacement with 2-propanol. N-Succinimidyl sulfoacetate tetraethylammonium salt was prepared from sulfoacetic acid treated with charcoal in aqueous solution, neutralized with an equimolar amount of tetraethylammonium hydroxide, and reacted with N-hydroxysuccinimide and 1,3-dicyclohexylcarbodiimide (DCC) at room temperature after changing water to dichloromethane. After removal of dicyclohexylurea and the excess of DCC by cold filtration and by washing with

hexane, respectively, the obtained active ester was used in the reaction with polyallylamine without any additional purification. N-Succinimidyl β-cholesteryloxyacetate was prepared by reacting N-hydroxysuccinimide and the corresponding acid in the presence of 1-ethyl-3-(3-dimethylaminopropyl)carbodiimide hydrochloride (EDC) in dichloromethane at room temperature and purified by crystallization from ethyl acetate (final yield - 80%). β-Cholesteryloxyacetic acid was synthesized by reacting cholesterol, lithium *tert*-butoxide and bromoacetic acid taken at a molar ratio of 1:4.7:2.5 in a mixture of N,N-dimethylacetamide and toluene (5.6:1 by volume, 7.15 ml of the solvent mixture per 1 mmole of cholesterol) at 50–55°C. After the reaction completion, the mixture was diluted with water, heated to reflux (to hydrolyze ester by-products) and acidified. The acid was purified by dissolution in chloroform followed by filtration through silica-gel and crystallization from heptane (final yield - 79%).

Nanoparticle Formulation

All formulations were prepared using the emulsification-solvent evaporation method modified to provide nanoparticles with controllable size, impregnated with nanocrystalline magnetite. To obtain smaller sized albumin-coated MNP (average diameter: 267±7 nm), 2.5 ml of ethanolic solution of ferric chloride hexahydrate and ferrous chloride tetrahydrate (170 and 62.5 mg, respectively) was added to an equivalent amount of sodium hydroxide dissolved in water (0.5 M, 5 mL). The precipitate was heated for 1 min at 90°C, cooled on ice, and separated on a magnet. The obtained magnetite was stirred with an ethanolic solution of oleic acid (150 mg) at 90°C for 5 min. Free oleic acid was separated by addition of deionized water. Oleic acid-coated magnetite was washed with ethanol, dispersed in 8 ml chloroform, and used to dissolve 90 mg of poly(D,L-lactide) and 10 mg of poly(D,L-lactide) covalently labeled with BODIPY$_{564/570}$. The organic dispersion was emulsified by sonication on ice in an aqueous solution of BSA (150 mg, 10 mL), and the organic solvent was removed under reduced pressure. Larger sized MNP (average diameter: 352± 6 nm) were prepared as above using two-fold larger amounts of oleic acid-coated magnetite, poly(D,L-lactide) and albumin, with the organic and aqueous phase volumes adjusted to 6 ml and 15 ml, respectively. MNP were washed twice with water by magnetic decantation, resuspended in 6 mL of aqueous trehalose (10% w/v), filtered (5.0 μm PVDF membrane, Millipore, MA, USA), and lyophilized.

MNP with affinity for Ad were formed via MNP surface modification with PAA-Chol-PDT-SO_3^- synthesized as above. The aqueous phase was prepared by dissolving 20 mg of PAA-Chol-PDT-SO_3^- in 15 ml water. The organic phase prepared as described for larger sized albumin-stabilized MNP was emulsified in the aqueous phase by sonication, and chloroform was removed under reduced pressure. MNP with an average size of 357±8 nm and 43% (w/w) magnetite loading were washed twice with water by magnetic decantation, modified with the thiolated human recombinant D1 domain of CAR as described elsewhere (13), and lyophilized with 10% trehalose. All lyophilized MNP formulations were kept at –80°C and resuspended in deionized water before use.

The size and iron oxide loading of MNP formulations were determined by dynamic light scattering and UV spectrophotometry, respectively, as previously published (14). Magnetic hysteresis curves of MNP and MNP-loaded cells were obtained using an alternating gradient magnetometer (Princeton Measurements Corporation, Princeton, NJ, USA).

Magnetically Driven MNP Sedimentation and Cell Uptake Kinetics

For sedimentation kinetics measurements albumin-stabilized MNP diluted to 45 μg MNP per ml in DMEM supplemented with 10% fetal bovine serum were applied to the wells of two 96-well plates (200 μl/well). One plate was positioned on a 96-well magnetic separator with an average field gradient of 32.5 T/m (LifeSep™ 96 F, Dexter Magnetic Technologies, Fremont, CA, USA), another was used for control measurements without magnetic exposure. The MNP suspensions were carefully removed at predetermined timepoints without disturbing the sedimented particles, and their fluorescence was measured in triplicates ($\lambda_{ex}/\lambda_{em}$= 540 nm/575 nm) to determine fractional depletion relative to initial MNP suspensions used as a reference. The mass balance was confirmed using sedimented MNP redispersed in 200 μl medium.

MNP uptake kinetics were determined in bovine aortic endothelial cells (BAEC) seeded at confluence on 96-well plates. Two hundred μl of MNP diluted to 1.8–9.0 μg/well with DMEM supplemented with 10% FBS were added to cells in triplicates with/without magnetic exposure as above. At predetermined timepoints cells were washed twice with 2% BSA in PBS to remove non-internalized MNP, observed under a fluorescent microscope, and their MNP loading determined fluorimetrically ($\lambda_{ex}/\lambda_{em}$=540 nm/575 nm). Cell viability was measured after Calcein AM staining ($\lambda_{ex}/\lambda_{em}$=485 nm/535 nm) in comparison to untreated cells.

Substrate Attachment of MNP-Loaded Cells Driven by a Magnetic Force Applied against Gravity

A 96-well plate with confluent BAEC was placed on the magnetic separator and incubated with 270 nm-sized MNP

(7.2 μg MNP/well) for 24 h. Untreated cells were used as a control. Cells were washed with PBS, detached with 1 mM EDTA solution in normal saline (15 min, 37°C), washed with PBS, resuspended in DMEM supplemented with 10% FBS, counted using a hemocytometer, and diluted to 10^5 cells/ml. Two hundred μl of the MNP-loaded and control cell suspensions were applied in sextuplicates to the wells of two 96-well plates. Both plates were carefully inverted with cell suspensions retained in the wells, and the magnetic separator was positioned upside down on top of one of the plates to create a magnetic field with its gradient applied in the direction opposite to that of gravitational force. After 1 h the cells were stained for viability with Calcein AM, observed under a fluorescent microscope, and counted.

Magnetically Driven Adenoviral Transduction of Endothelial Cells

D1-coated MNP and $_{GFP}$Ad were diluted in 5% glucose solution, combined at varying ratios to form MNP-$_{GFP}$Ad affinity complexes as described elsewhere (15), and after 15 min applied to confluent BAEC seeded on 96-well plates at doses corresponding to 0–2.2 μg MNP and 0–6.7×10^7 viral particles per well. One plate was positioned on the magnetic separator. After 20 min the cells were washed twice with 2% BSA in PBS and incubated with fresh DMEM supplemented with 10% FBS. To determine the uptake and GFP expression, the medium was replaced with PBS and the fluorescent signal was assayed in live cells 24 h post treatment using $\lambda_{ex}/\lambda_{em}$ of 540 nm/575 nm and 485 nm/535 nm, respectively. BAEC treated with affinity complex formulations without the magnetic exposure were included as controls.

Statistical Analysis

Experimental data were expressed as means ± standard deviations. The results were evaluated by Kruskal–Wallis one-way ANOVA with Dunn's post hoc analysis or Mann-Whitney Rank Sum Test. Cell transduction data were analyzed by regression coefficients' comparison. Differences were termed significant at $P<0.05$.

RESULTS

The effect of the size and magnetic responsiveness of albumin-stabilized biodegradable MNP on their cell uptake and toxicity in cultured endothelial cells was examined using polylactide-based MNP formulated with a narrow size distribution and average diameters of 267±7 nm and 352±6 nm (Fig. 1a) using a modification of the emulsification-solvent evaporation method providing albumin-stabilized, superparamagnetic MNP with adjustable size. The two formulations were obtained with magnetite loadings of 38% and 43% w/w for the smaller and larger sized MNP, respectively, consistent with their weight-normalized saturation magnetization values (14.2 and 16.0 emu/g, Fig. 1b). The composite design of MNP, where multiple individual small-sized magnetite nanocrystals are incorporated in the rigid particle matrix formed by PLA, is essential for both the strong magnetic responsiveness and negligible magnetic remanence (0.71±0.04% of the respective saturation values for both MNP formulations, Fig. 1b) (15,16). The expected ratio of the magnetic responsiveness of individual particles in the two formulations based on the differences in their linear dimensions and magnetite loadings averages ~2.3 in proportion to the respective amounts of magnetite in their composition. In agreement with their significantly stronger magnetic susceptibility larger sized MNP exhibited a notably higher sedimentation rate in the presence of a high-gradient magnetic field (Fig. 1c). The sedimentation kinetics reveal a biphasic pattern with 58.8±0.3% and 33.4±0.9% of larger and smaller-sized MNP, respectively, depleted from suspension under magnetic conditions within 2 min, and with slower sedimentation rates observed with both formulations at later timepoints (first 30 min shown in detail in Fig. 1d), suggesting the existence of a "rapid depletion zone" wherein the particle motion is dominated by the magnetic force. The rapid capture of larger and smaller MNP occurs at respective average distances of 4.81±0.02 mm and 3.28±0.05 mm from the surface of the magnet where the magnetic field gradient is maximal (32.5 T/m), as calculated based on their fractional depletion, height of liquid in the well and well bottom thickness, assuming uniform initial distribution of MNP in suspension. At later time points the sedimentation kinetics reflect the significantly slower rates at which particles initially located at larger distances from the magnet enter the rapid depletion zone driven by a combined effect of the magnetic attraction, Brownian motion and gravity. Interestingly, in the absence of the magnetic exposure the sedimentation of larger sized MNP was complete after 24 h compared to 60±6% of smaller MNP remaining in suspension by this timepoint.

A fraction of each type of MNP internalized by cultured endothelial cells at a given timepoint with exposure to a high-gradient field was independent of the applied MNP dose in the studied dose range (1.8–9.0 μg/well, Figs. 2a and b and 3e and f), as proportionately higher absolute amounts of MNP were internalized by cells treated with increasing MNP doses. As expected based on their magnetic susceptibilities, the kinetic rates of the MNP uptake under magnetic conditions were a direct function of the MNP size (73±4 *vs.* 26±2% of larger and smaller sized MNP, respectively, internalized after 8 h). Smaller sized MNP exhibited near-constant uptake rates, whereas the internalization of larger

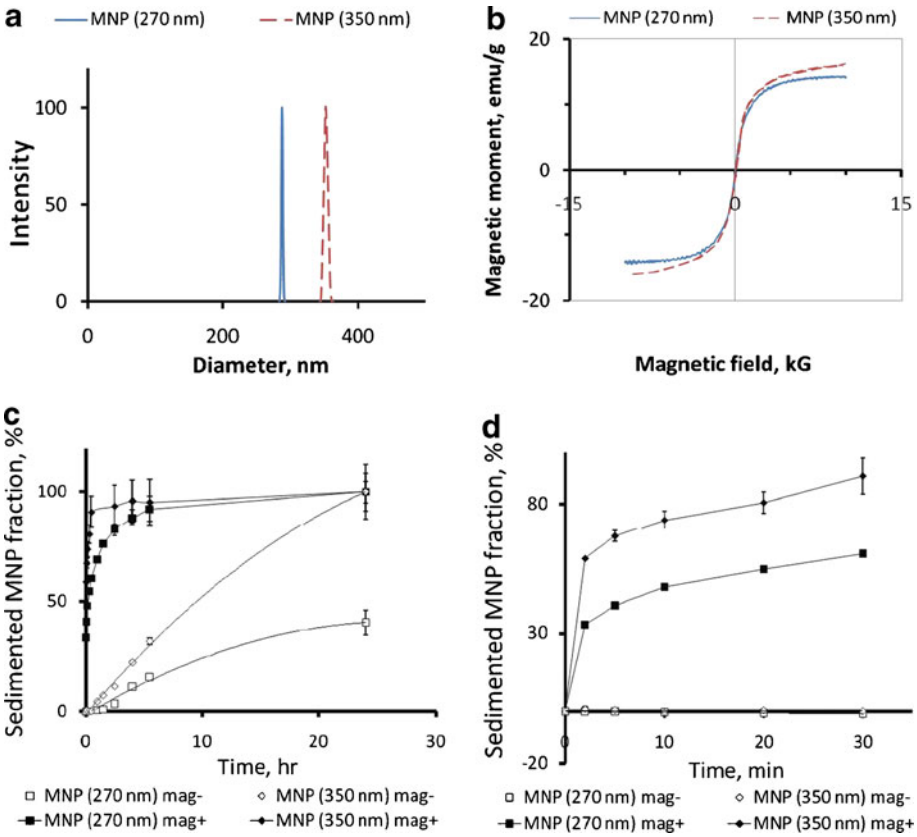

Fig. 1 Physical properties and sedimentation kinetics of biodegradable MNP formulations. Particle size distribution of smaller and larger sized MNP formulations (270 nm and 350 nm) was determined by dynamic light scattering (**a**), and their magnetization curves (**b**) were obtained using an alternating gradient magnetometer (Princeton Measurements). Sedimentation rates of $BODIPY_{564/570}$-labeled MNP as a function of MNP size and exposure to a high-gradient magnetic field were measured by fluorimetry (**c**, $\lambda_{ex}/\lambda_{em}$=540 nm/575 nm). The fractional sedimentation kinetics in the first 30 min are shown in more detail in **d**.

MNP followed a saturation pattern (Fig. 2a and b), with respective internalized fractions of 84±7% and 97±3% at 24 h. Notably, in contrast to MNP sedimentation occurring at measurable rates in the absence of a magnetic force, the high-gradient field was essential for achieving efficient MNP internalization (2.2±0.2% and 10.7±1.1% of smaller and larger sized MNP internalized by the 24 h timepoint without the magnetic exposure, See Fig. 2c and d, and Fig. 3c *vs.* a and d *vs.* b), suggesting that the magnetic force-mediated enhancement of cellular uptake observed with these formulations is not fully accounted for by accelerated deposition of MNP on the cell surface. MNP not removable by washing with 2% BSA in PBS exhibited perinuclear localization characteristic of endocytosed particles at all timepoints, with smaller sized MNP distributed more uniformly in comparison to larger particles showing alignment in chain-like structures immediately after removal of the high-gradient field (See images taken after 24 h of cell exposure to MNP at a dose of 7.2 μg/well, shown in Fig. 3a and b, respectively), as previously demonstrated by Wilhelm *et al.* (17). The viability of cells treated for 24 h with smaller and larger sized MNP under magnetic conditions in comparison to untreated cells was 83±5% and 75±0% for the dose of 9 μg/well and 93±0% and 83±2% for 7.2 μg/well, respectively (Fig. 3g, h). This decrease in cell viability was inversely dependent on the amount of MNP endocytosed under respective conditions, suggesting that an optimized cell loading procedure can provide acceptable cell viability (>90%) at MNP loading corresponding to ~160 pg iron oxide per cell. Hysteresis measurements showed saturation magnetization of 0.89 and 1.05 nemu/cell after magnetically driven cell loading for 24 h with 7.2 μg/well of smaller and larger sized MNP. The remnant magnetization and coercive force values were 0.10 and 0.12 nemu/cell and 4.1 and 4.4 mOe/cell, respectively, in agreement with the low residual magnetization exhibited by the MNP formulations (Fig. 1b).

In addition to the obvious requirement for the absence of cell toxicity, the treatment with MNP should not adversely affect the capacity of magnetically guided endothelial cells to rapidly attach to substrate, a prerequisite for their effective homing to the target site (11). These studies addressed cell-substrate attachment of MNP-loaded cells driven by a magnetic force applied in a direction opposite to that of gravity. An experiment with MNP-loaded BAEC applied in suspension to a 96-well plate, which was carefully inverted and then covered with a magnetic separator magnet positioned upside-down ('inverted plate' experiment) showed 91±12% of the initially taken number of cells exhibiting attachment and spreading on the inverted substrate in the presence of a high-gradient field applied for 1 h (Fig. 4). Attaching cells exhibited a perinuclear pattern of MNP distribution (Fig. 4a, b). Calcein staining confirmed the viability of the attached cells unaffected in the course of the experiment (Fig. 4c). Untreated or MNP-loaded BAEC incubated in the wells of inverted plates with or without

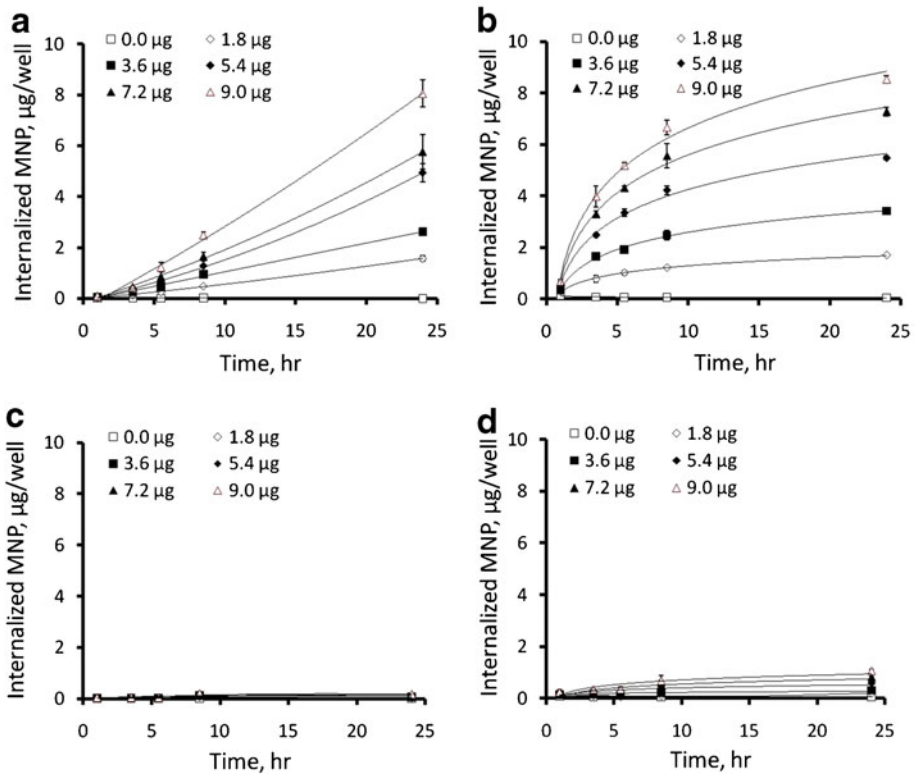

Fig. 2 Cell uptake kinetics in BAEC determined for 270 nm (**a**, **c**) and 350 nm sized MNP (**b**, **d**). The internalization kinetics were measured fluorimetrically ($\lambda_{ex}/\lambda_{em}$=540 nm/575 nm) in confluent cells incubated with MNP in the presence of a high-gradient magnetic field (**a**, **b**), or without the magnetic exposure (**c**, **d**) as a function of MNP dose.

a high-gradient magnetic field, respectively, exhibited substrate attachment <4%, significantly lower than that of MNP-loaded BAEC under magnetic conditions (P=0.003, Fig. 4d–j).

Cell loading with MNP may be accomplished *ex vivo* simultaneously with genetic cell modification to provide an integrated, magnetically targeted cell/gene delivery strategy

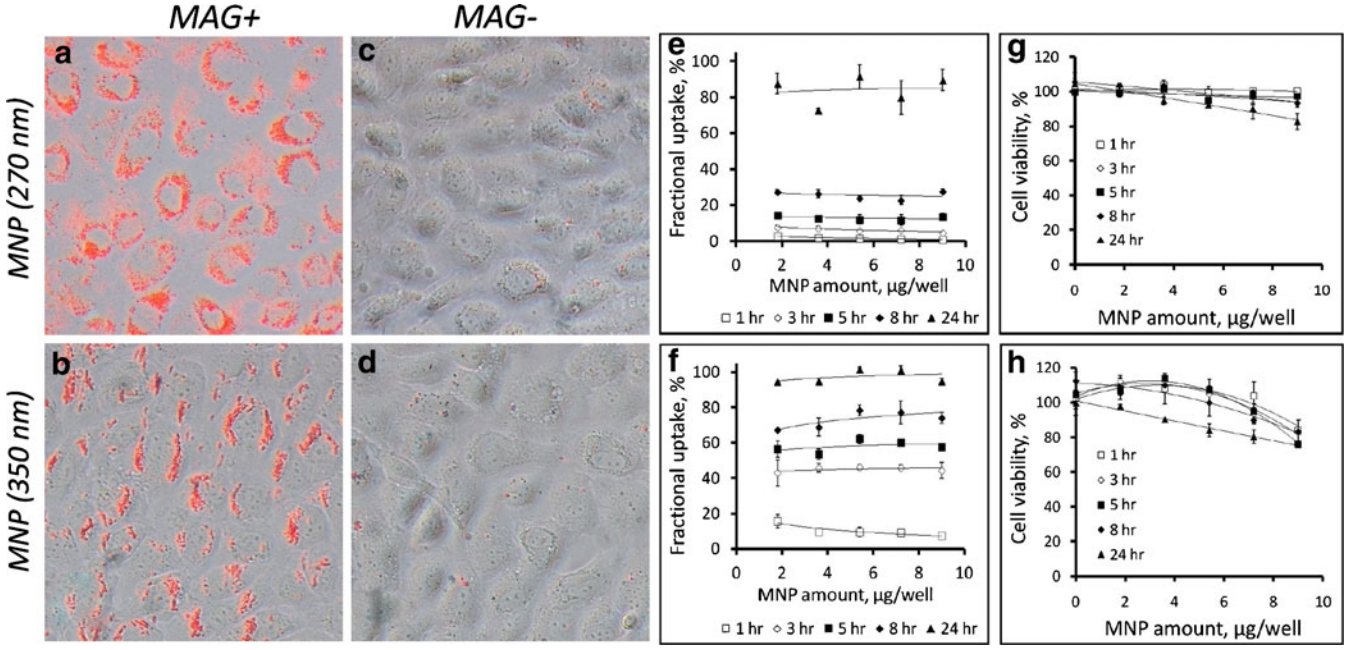

Fig. 3 MNP cellular localization and effect on cell viability. Merged red fluorescent and bright field images show cellular localization of MNP ((**a**, **c**) 270 nm MNP; (**b**, **d**) 350 nm MNP) in bovine aortic endothelial cells after 24 h incubation with MNP formulations at 7.2 μg/well in the presence of a high-gradient magnetic field (**a**, **b**) or without the magnetic exposure (**c**, **d**) observed by fluorescent microscopy (Original magnification × 400). Dose efficiency of MNP uptake under magnetic conditions from data shown in Fig. 2 is presented in E and F as a fraction of the MNP dose internalized by cells (**e**) 270 nm MNP; (**f**) 350 nm MNP). Cell viability was measured in magnetically treated cells as a function of formulation type ((**g**) 270 nm MNP; (**h**) 350 nm MNP), MNP dose and magnetic exposure duration by fluorimetry after cell staining with Calcein AM ($\lambda_{ex}/\lambda_{em}$=485 nm/535 nm).

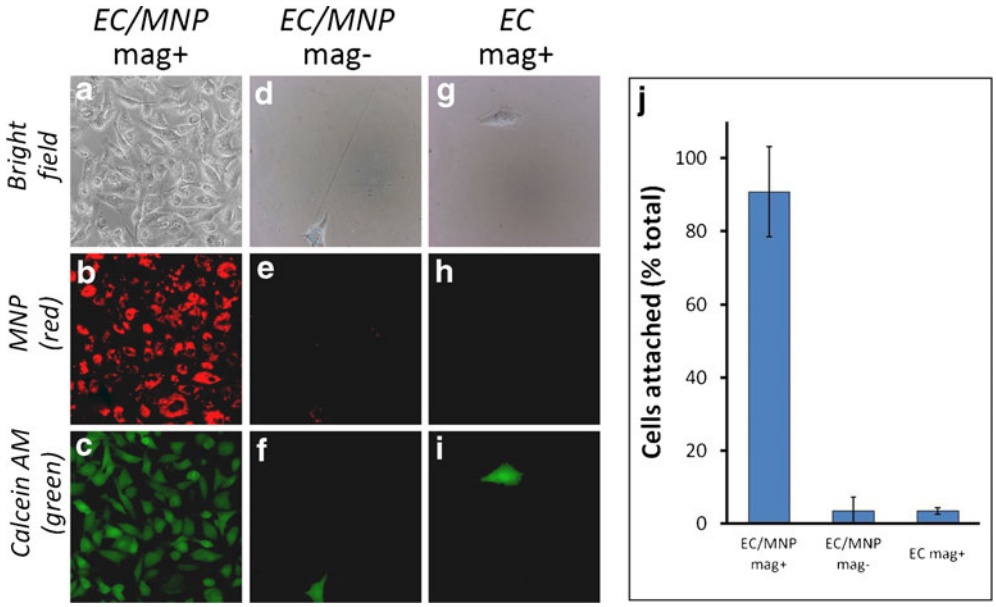

Fig. 4 Magnetically driven attachment and viability of MNP-loaded cells. Confluent BAEC were incubated with 270 nm MNP in the presence of a high-gradient magnetic field for 24 h to provide average MNP loading equivalent to 160 pg iron oxide per cell. Suspensions of MNP-loaded cells (EC/MNP, **a**–**f**) or untreated cells used as a control (EC, **g**–**i**) were applied to wells of two 96-well plates, the plates were carefully flipped, and a magnetic separator was positioned upside down on top of one of the plates to provide a magnetic field with its gradient applied in the direction opposite to that of the gravitational force. After 1 h the cells were stained with Calcein AM, observed by fluorescent microscopy for morphology (**a**, **d**, **g**), MNP (**b**, **e**, **h**) and viability (**c**, **f**, **i**), and counted to obtain the fraction of initially taken cells exhibiting stable substrate attachment under the experimental conditions (**j**).

(6,10,15). This combination can be achieved by using MNP formulations capable of forming stable complexes with gene delivery vectors (6,14,15,18–20). In this study we used MNP (average size 357±8 nm) modified with a novel trifunctional surface-active polymer (Fig. 5) allowing surface attachment of the adaptor protein, a recombinant D1 domain of CAR with strong affinity for Ad (13,21). The polymer with a high surface activity was designed with a hydrophobic cholesteryl moiety that provides efficient anchorage to the MNP surface, a charged sulfonate group electrostatically stabilizing the particles in suspension, and a thiol-reactive pyridyldithio function enabling covalent attachment of the D1 adaptor. Both the cell uptake and gene transfer efficiency of the complexes were essentially dependent on the magnetic exposure (Fig. 6a–f). BAEC incubated for 20 min with MNP complexed with $_{GFP}$Ad [MNP($_{GFP}$Ad)] in the presence of the high-gradient field showed significantly higher levels of GFP expression compared to non-magnetic conditions or free Ad (Fig. 6b, d and f, $P \ll 0.001$ for all studied MNP doses), while the viability of the cells measured 24 h after their magnetic or non-magnetic exposure to the affinity complexes formed at all studied ratios of MNP and Ad was ≥90% in comparison to untreated cells used as a control. The GFP expression levels in magnetically treated cells were directly dependent on the amounts of both MNP and Ad (Fig. 6g). Notably, the amount of complexes taken up by cells was directly proportionate to the MNP dose, but equally efficient for all studied MNP to Ad ratios, averaging 59.5±0.5% *vs.* 3.8±1.3% of the total amount of MNP applied with or without a magnetic exposure, respectively (P=0.008). Thus, in contrast to electrosterically stabilized albumin-coated MNP, a brief exposure to the high-gradient field was sufficient for achieving stable cell binding and subsequent endocytosis of the charge-stabilized MNP in agreement with similar findings reported for a different type of strongly charged formulations (22).

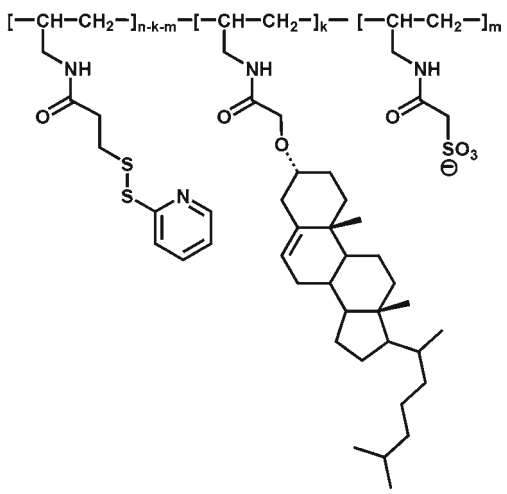

Fig. 5 Structure of the surface-active agent (PAA-Chol-PDT-SO_3^-, n=100, k=0.12n, m=0.35n) used for colloidal stabilization and chemical modification of MNP to enable formation of MNP affinity complexes with adenovirus.

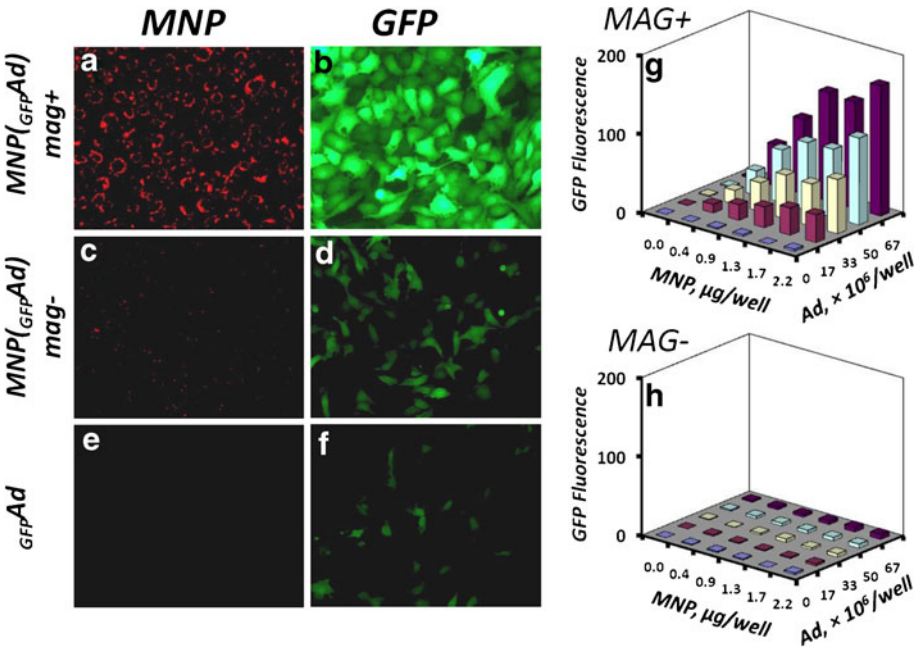

Fig. 6 Cell uptake and *in vitro* transduction efficiency of MNP-Ad affinity complexes in cultured BAEC. Cells seeded at confluence were incubated for 20 min with MNP affinity complexes formed with type 5 Ad encoding GFP in the presence of a high-gradient magnetic field (**a**, **b**) or without the magnetic exposure (**c**, **d**) in comparison to free Ad (**e**, **f**). MNP uptake and GFP expression were observed after 24 h by fluorescent microscopy (original magnification × 200). Transduction efficiency was determined fluorimetrically ($\lambda_{em}/\lambda_{ex}$=485 nm/535 nm) as a function of the magnetic exposure (**g** *vs.* **h**), and the doses of MNP and Ad. Each data point represents an average of three experimental replicates. MNP complexes with $_{GFP}$Ad resulted in significantly higher levels of GFP expression when applied in the presence of a high-gradient field compared to non-magnetic conditions or free Ad ($P \ll 0.001$ for all studied MNP doses).

DISCUSSION

In order to be clinically applicable, a cell therapeutic strategy should efficiently confine cells to their target site and enable high rates of engraftment without adversely affecting cell functionality. Novel magnetic targeting designs making externally controlled delivery of magnetically responsive agents to non-superficial sites in the body possible (10,23,24) can potentially be applied to achieve accelerated recovery of functional endothelium and healing of injured blood vessels in cardiovascular disease patients via site-specific delivery of endothelial cells. The formulation and characteristics of MNP used for endothelial cell modification are one of the critical determinants of the efficiency of targeted cell therapy. Properly designed MNP should: 1) have no adverse effects on cell viability; 2) consist of components that can be fully degraded or excreted; 3) exhibit strong magnetic responsiveness in absence of remanent magnetization; 4) be efficiently and rapidly internalized by cells *ex vivo*. The requirement for MNP biocompatibility has prompted interest in exploring the utility of injectable iron oxide nanoparticle formulations already used clinically (5,11). However, as shown recently with Endorem™, the onset of significant cell toxic effects may already be evident at magnetic loadings >4 pg iron oxide per cell (5). Furthermore, these ready-made formulations can not be used for elucidating the effect of specific formulation variables on the cell loading process. Thus, a need remains for developing formulation procedures that can be applied to make MNP with controllable physical properties enabling efficient generation of strongly magnetically responsive endothelial cells without adversely affecting their viability and capacity for stable binding to the target site post delivery.

This study addresses uptake kinetics and cell compatibility of composite, PLA-based MNP formulations as a function of their size, exposure to a high-gradient magnetic field, and MNP dose. Two MNP formulations with different average sizes and uniform size distributions were prepared using a modification of the emulsification-solvent evaporation approach (16) from fully biodegradable components, including PLA as the matrix-forming material, nanocrystalline magnetite as the magnetically responsive ingredient with negligible magnetic remanence, and albumin as a non-immunogenic and non-toxic surface stabilizer. Larger-sized MNP were produced by adjusting the concentrations of the particle-forming components in the organic phase to increase its viscosity. This in turn results in formation of larger precursor droplets as shown for nanoparticle formulation procedures involving emulsification and polymer precipitation steps (25,26). The 1.3-fold difference in the average diameters (352 nm *vs.* 267 nm) translates into a >2-fold larger payload of magnetite and a respectively

higher magnetic responsiveness of individual particles, which is reflected by different sedimentation rates of larger and smaller MNP in the presence of a high-gradient magnetic field. While both formulations exhibited a biphasic sedimentation pattern under magnetic conditions, the rapid capture of the MNP located within the range where their motion is dominated by the magnetic force (rapid depletion zone) affected a considerably larger fraction of the 350 nm-sized MNP. The corresponding distance from the magnet surface can be readily obtained from the ratio of particles depleted at the earliest timepoint to the initial particle amount, and may provide a useful tool for comparing average magnetic responsiveness of individual particles in different MNP formulations.

The uptake kinetics examined in comparison to the sedimentation rates suggest that the magnetically driven deposition on the cell surface, while essential for MNP internalization, may not be the rate-limiting process for the both albumin-stabilized MNP formulations. While the sedimentation of the two MNP formulations was near-complete after 4 h, their cell uptake after this timepoint proceeded at highly different rates, with larger sized MNP showing more efficient internalization over time. Thus, the deposition of albumin-coated MNP is not sufficient for their stable association with the cell surface and initiation of endocytosis, which requires continuous application of the magnetic force beyond the completion of the sedimentation phase and occurs at a rate directly dependent on the individual magnetic responsiveness of the particles. Interestingly, the dose efficiency of MNP uptake in the presence of a high-gradient field, expressed as a fraction of the MNP dose internalized by cells by a given time, while showing a direct dependence on the particle size (350 nm-sized MNP being superior at all timepoints in comparison to 270 nm-sized MNP), did not exhibit dependence on the MNP dose itself. This suggests that the magnetically enhanced uptake of the both formulations does not reach saturation of the endocytosis pathway within the studied MNP dose range. The acceptable dose of MNP may however be limited by the viability and capacity for substrate attachment of MNP-loaded cells post treatment, and was found to be equivalent to ~160 pg iron oxide per cell in these studies. An efficient magnetic cell targeting strategy is expected to not only guide MNP-loaded cells and concentrate them at the target site, but also promote their stable homing and retention after delivery. Of note, endothelial cells impregnated with MNP at 160 pg iron oxide per cell demonstrated efficient attachment and spreading after a 1 h incubation driven by a magnetic force applied against gravity. Additional studies examining the proliferation rates of MNP-loaded endothelial cells and the kinetics of the MNP elimination are required for establishing the long-term cell compatibility of these MNP formulations.

Magnetically targeted delivery of genetically modified cells expressing therapeutically relevant transgenes can potentially provide an effective combination strategy (10,23). Cell transduction can be accomplished concomitantly with magnetic loading using MNP formulated with capacity for magnetically driven gene transfer (6,15). In this study we investigated the *in vitro* transduction efficiency of magnetically responsive affinity complexes formed between MNP and Ad. PLA-based MNP were formulated using a novel polymer with enhanced surface-active properties used as a colloidal stabilizer and a source of thiol reactive functions for subsequent particle surface modifications. The high surface activity and strong negative charge of the polymer resulted in its stable association with the particle surface without the need for covalent attachment utilized in our previous studies (13,15). MNP surface-modified with recombinant D1 protein as an affinity adaptor molecule demonstrated efficient cell binding and endocytosis in cultured endothelial cells in the presence of a high-gradient field. The affinity functionalization of the particles has been shown to be essential for providing high levels of magnetically driven adenoviral gene transfer as demonstrated previously by comparing the transduction capacity of MNP covalently modified with D1 *vs.* non-immune IgG and applied to endothelial cells in combination with Ad (15). Consistent with these findings, Ad affinity complexes with MNP functionalized in the present study using the novel, non-covalent strategy and applied to cells in the presence of the high-gradient magnetic field resulted in high transgene expression levels significantly exceeding those observed with free Ad. Notably, the transduction levels and the resultant magnetic responsiveness of cells can be optimized simultaneously by adjusting the respective amounts of MNP and Ad used to form the affinity complexes.

CONCLUSIONS

These studies characterized the physical properties of biodegradable, PLA-based MNP formulated with controllable size and a high loading of superparamagnetic nanocrystalline magnetite, demonstrated the applicability of these MNP formulations for rapid and dose-efficient, magnetically driven loading of endothelial cells, and established the threshold of MNP loading achievable without adversely affecting cell viability and capacity for substrate binding, a prerequisite for stable cell homing to the target site after magnetic delivery. The presence of a high-gradient field was found to be essential for rapid MNP internalization, and the kinetic rates of cell uptake were shown to be directly dependent on particle size and incubation time. The difference between the internalization efficiencies of the smaller and larger sized MNP is not fully accounted for by the respective

sedimentation rates, suggesting that cell surface binding rather than accelerated sedimentation is rate limiting in the MNP loading process. In addition, PLA-based MNP enabling a combination of magnetic loading and enhanced transduction of endothelial cells were formulated using a new surface modification strategy and shown to provide efficient magnetically driven gene transfer *in vitro*. Additional studies focusing on pathways and kinetics of MNP elimination, and the comparative effect of cell loading with MNP on their capacity for proliferation are required for optimizing MNP formulations and confirming their applicability for producing fully functional magnetically responsive cells for targeted delivery applications.

ACKNOWLEDGMENTS & DISCLOSURES

This research was supported in part by grants from the NIH (HL72108 and HL94816), the American Heart Association (Scientist Development Grant 10SDG4020003), the Nanotechnology Institute and the William J. Rashkind Endowment of The Children's Hospital of Philadelphia.

REFERENCES

1. Schlorf T, Meincke M, Kossel E, Gluer CC, Jansen O, Mentlein R. Biological properties of iron oxide nanoparticles for cellular and molecular magnetic resonance imaging. Int J Mol Sci. 2011;12(1):12–23.
2. Sykova E, Jendelova P, Herynek V. MR tracking of stem cells in living recipients. Methods Mol Biol. 2009;549:197–215.
3. Pislaru SV, Harbuzariu A, Agarwal G, Witt T, Gulati R, Sandhu NP, *et al.* Magnetic forces enable rapid endothelialization of synthetic vascular grafts. Circulation. 2006;114(1 Suppl):I314–8.
4. Pislaru SV, Harbuzariu A, Gulati R, Witt T, Sandhu NP, Simari RD, *et al.* Magnetically targeted endothelial cell localization in stented vessels. J Am Coll Cardiol. 2006;48(9):1839–45.
5. Kyrtatos PG, Lehtolainen P, Junemann-Ramirez M, Garcia-Prieto A, Price AN, Martin JF, *et al.* Magnetic tagging increases delivery of circulating progenitors in vascular injury. JACC Cardiovasc Interv. 2009;2(8):794–802.
6. Hofmann A, Wenzel D, Becher UM, Freitag DF, Klein AM, Eberbeck D, *et al.* Combined targeting of lentiviral vectors and positioning of transduced cells by magnetic nanoparticles. Proc Natl Acad Sci U S A. 2009;106(1):44–9.
7. Polyak B, Fishbein I, Chorny M, Alferiev I, Williams D, Yellen B, *et al.* High field magnetic gradients can target magnetic nanoparticle-loaded endothelial cells to the surfaces of steel stents. Proc Natl Acad Sci U S A. 2008;105(2):698–703.
8. Shimizu K, Ito A, Arinobe M, Murase Y, Iwata Y, Narita Y, *et al.* Effective cell-seeding technique using magnetite nanoparticles and magnetic force onto decellularized blood vessels for vascular tissue engineering. J Biosci Bioeng. 2007;103(5):472–8.
9. Muthana M, Scott SD, Farrow N, Morrow F, Murdoch C, Grubb S, *et al.* A novel magnetic approach to enhance the efficacy of cell-based gene therapies. Gene Ther. 2008;15(12):902–10.
10. Fishbein I, Chorny M, Levy RJ. Site-specific gene therapy for cardiovascular disease. Curr Opin Drug Discov Devel. 2010;13(2):203–13.
11. Soenen SJ, Himmelreich U, Nuytten N, De Cuyper M. Cytotoxic effects of iron oxide nanoparticles and implications for safety in cell labelling. Biomaterials. 2010;32(1):195–205.
12. Nyanguile O, Dancik C, Blakemore J, Mulgrew K, Kaleko M, Stevenson SC. Synthesis of adenoviral targeting molecules by intein-mediated protein ligation. Gene Ther. 2003;10(16):1362–9.
13. Chorny M, Fishbein I, Alferiev IS, Nyanguile O, Gaster R, Levy RJ. Adenoviral gene vector tethering to nanoparticle surfaces results in receptor-independent cell entry and increased transgene expression. Mol Ther. 2006;14(3):382–91.
14. Chorny M, Polyak B, Alferiev IS, Walsh K, Friedman G, Levy RJ. Magnetically driven plasmid DNA delivery with biodegradable polymeric nanoparticles. FASEB J. 2007;21(10):2510–9.
15. Chorny M, Fishbein I, Alferiev I, Levy RJ. Magnetically responsive biodegradable nanoparticles enhance adenoviral gene transfer in cultured smooth muscle and endothelial cells. Mol Pharm. 2009;6(5):1380–7.
16. Chorny M, Fishbein I, Yellen BB, Alferiev IS, Bakay M, Ganta S, *et al.* Targeting stents with local delivery of paclitaxel-loaded magnetic nanoparticles using uniform fields. Proc Natl Acad Sci U S A. 2010;107(18):8346–51.
17. Wilhelm C, Gazeau F, Bacri JC. Rotational magnetic endosome microrheology: viscoelastic architecture inside living cells. Phys Rev E Stat Nonlin Soft Matter Phys. 2003;67(6 Pt 1):061908.
18. Tresilwised N, Pithayanukul P, Mykhaylyk O, Holm PS, Holzmuller R, Anton M, *et al.* Boosting oncolytic adenovirus potency with magnetic nanoparticles and magnetic force. Mol Pharm. 2010;7(4):1069–89.
19. Tresilwised N, Pithayanukul P, Holm PS, Schillinger U, Plank C, Mykhaylyk O. Effects of nanoparticle coatings on the activity of oncolytic adenovirus-magnetic nanoparticle complexes. Biomaterials. 2012;33(1):256–69.
20. Mah C, Fraites Jr TJ, Zolotukhin I, Song S, Flotte TR, Dobson J, *et al.* Improved method of recombinant AAV2 delivery for systemic targeted gene therapy. Mol Ther. 2002;6(1):106–12.
21. Chorny M, Fishbein I, Levy RJ. Endothelial cells transduced with magnetically responsive nanoparticles formulated with iNOS encoding adenovirus inhibit proliferation of aortic smooth muscle cells in a direct co-culture model. Mol Ther. 2009;17:S393.
22. Huth S, Lausier J, Gersting SW, Rudolph C, Plank C, Welsch U, *et al.* Insights into the mechanism of magnetofection using PEI-based magnetofectins for gene transfer. J Gene Med. 2004;6(8):923–36.
23. Chorny M, Fishbein I, Forbes S, Alferiev I. Magnetic nanoparticles for targeted vascular delivery. IUBMB Life. 2011;63(8):613–20.
24. Kempe H, Kates SA, Kempe M. Nanomedicine's promising therapy: magnetic drug targeting. Expert Rev Med Devices. 2011;8(3):291–4.
25. Astete CE, Sabliov CM. Synthesis and characterization of PLGA nanoparticles. J Biomater Sci Polym Ed. 2006;17(3):247–89.
26. Chorny M, Fishbein I, Danenberg HD, Golomb G. Lipophilic drug loaded nanospheres prepared by nanoprecipitation: effect of formulation variables on size, drug recovery and release kinetics. J Control Release. 2002;83(3):389–400.